Published in final edited form as:
J Neurosci Res. 2009 April ; 87(5): 1250–1259. doi:10.1002/jnr.21921.

Cyclophilin D is predominantly expressed in mitochondria of GABAergic interneurons

Julie L. Hazelton, **Maryna Petrasheuskaya**, **Gary Fiskum**, and **Tibor Kristián**
Department of Anesthesiology Research, School of Medicine, University of Maryland, Baltimore, MD 21201

Abstract

Brain mitochondria are relatively resistant to calcium-induced mitochondrial permeability transition (MPT) with heterogenic response to the insult. Since the cause for this heterogeneity is not clear we studied the distribution of a key regulator of the MPT, cyclophilin D (cypD) within the rat brain by using immunohistology and western blotting. Motor and parietal cortex, hippocampus, striatum, substantia nigra, ventral tegmental area, septum, and mammillary nucleus displayed a strong immunoreactivity to cypD within specific subpopulation of neurons. The staining was punctate and intense particularly in perinuclear regions of cells. Apart from neurons, a subpopulation of astrocytes and NG2 positive cells showed higher cypD immunoreactivity. The double staining of cypD with cytochrome oxidase confirmed the mitochondrial specificity of cypD immunoreactivity. The neurons with high levels of cypD also expressed glutamate decarboxylase (GABA) and the calcium binding protein parvalbumin or calbinding D-28k, identifying these cells as interneurons. Western blots confirmed our immunohistochemical findings showing significantly higher levels of cypD in crude mitochondria of substantia nigra when compared to cortex or striatum. Furthermore, nonsynaptic mitochondria representing mainly mitochondria from cell bodies of neurons and glia have about 16 % higher levels of cypD when compared to synaptic mitochondria that are localized in pre-synaptic buttons. These data suggest that the underlying factor of heterogenic response of isolated brain mitochondria to MPT-inducing insults can be the different expression levels of cypD with mitochondria originated from interneurons as the most sensitive.

Keywords

cyclophilin D; calcium-binding proteins; interneurons; mitochondria; brain

Introduction

Mitochondria have a fundamental role in regulating both apoptotic and necrotic cell death predominantly through the formation of the permeability transition pore (PTP). The opening of this pore is regulated by the mitochondrial protein cyclophilin D (cypD) (Bernardi et al. 1992; Halestrap and Davidson 1990). Cyclophilins represent a subgroup of a large family of enzymes called peptidyl cis-trans isomerases (PPI) that bind the immunosuppressant cyclosporine A (CsA) and catalyze the cis-trans isomerization of peptide bonds preceding proline residues (Schmid 1993, 1995). A physiological role for PPIases as catalysts of cellular protein folding reactions and a possible relation to molecular chaperones has been

Address correspondence to: Tibor Kristian, PhD, Department of Anesthesiology, School of Medicine, University of Maryland, 685 W Baltimore St, 534 MSTF, Baltimore, Maryland 21201, USA, Voice: (410) 706-3418, Fax: (410) 706-2550, E-mail: tkris001@umaryland.edu.

suggested (for reviews see Gothel and Marahiel 1999). Cyclophilin D is a mitochondrially-targeted cyclophilin, which has been implicated in accelerating the folding of newly imported protein into mitochondria (Matouschek et al. 1995, Rospert et al. 1996) and in regulation of a mitochondrial permeability transition (MPT) pore assembly.

It is commonly accepted that activation of MPT is a result of the interaction and conformational changes of several mitochondrial proteins (for review see (Crompton 2003). This process is catalyzed by cypD that is localized in the matrix. Initial evidence supporting the idea that cypD plays a direct role in the MPT emerged from an examination of the ability of CsA to inhibit PPIase activity, which correlated with inhibition of the MPT (Griffiths and Halestrap 1991, Connern and Halestrap 1992). Finally, purification of CsA binding proteins from total mitochondrial extracts by CsA affinity chromatography demonstrated that only cypD could be specifically eluted (Nicolli et al. 1996). The sensitivity of mitochondria to calcium-induced MPT is dependent on the expression levels of cypD (Brustovetsky et al. 2003, Eliseev et al. 2006). Thus, cypD is likely a key regulator of MPT activity. Recent studies using cypD null mice revealed the essential role of this protein and the MPT in necrotic cell death caused by calcium overload and oxidative stress (Basso et al. 2005, Li et al. 2004).

The MPT opening probability is modulated by several factors and drugs (Gunter and Pfeiffer 1990), but most importantly, calcium. Furthermore, the mitochondrial response to calcium-induced MPT has tissue-specific characteristics (Brustovetsky and Dubinsky 2000; Dubinsky et al. 1999, Kristal and Dubinsky 1997, Kristal et al. 2000, Kristal et al. 2001). Unlike mitochondria of liver or heart origin, brain mitochondria are relatively resistant to calcium-induced swelling (Andreyev and Fiskum 1999, Berman et al. 2000, Eliseev et al. 2006). When swelling of brain mitochondria was examined, a clear-cut heterogeneity in response to calcium was revealed (Kristian et al. 2000, 2001, 2002). Although a small subpopulation of brain mitochondria showed typical characteristics of swelling and some mitochondria were without significant morphological alterations, the majority of mitochondria displayed shrunken matrices with expansion of the inter-membrane space (Kristian et al. 2002, 2007). The mechanisms underlying this heterogenic response are elusive, however it could result from differential cypD expression levels in neurons and glia or within different brain regions.

We hypothesize that the cypD expression is heterogeneous within different brain regions or cells types. Therefore, in the present study we examined cypD distribution in the adult rodent brain. Immunohistochemistry and immunoblotting techniques were utilized to detect this protein in different cell-types of the brain and in isolated mitochondria from specific brain regions.

Materials and Methods

Animals and fixation

Five naïve adult (300g) male Fisher 344 rats were deeply anesthetized with ketamine and transcardially perfused with 4% paraformaldehyde. Brains were removed from the skull and transferred into 30% sucrose. Once the brains sunk to the bottom of the container, they were cut (30 μm) on a freezing sliding microtome and kept in cryoprotectant (−20°C) until further processing was initiated (Watson et al. 1986).

Nickel-diaminobenzidine tetrahydrochloride (NiDAB) visualization of cypD

Sections were rinsed multiple times in 0.05 M potassium phosphate-buffered saline (KPBS) buffer before and after exposure to a 1% solution of sodium borohydride for 20 min; primary antibody for 48 hr (MitoSciences, anti-cyclophilin D, 1:80,000); goat anti-mouse

secondary antibody (1:600) for 1 hr; and avidin biotin complex (1:222) solution for 1 hr. Tissue was rinsed before and after a 12 min incubation in NiDAB solution with 0.175 M sodium acetate buffer.

Double-labeling immunofluorescence

Sections were processed as described above with the addition of a blocking step against endogenous avidin biotin activity immediately prior to incubation in the primary antibody (anti-cypD, 1:50,000) for 48 hr. Tissue was then rinsed with KPBS before and after incubation in goat anti-mouse secondary antibody (1:5,000, 60 min), avidin biotin complex solution (1:444, 30 min), biotinylated tyramide (1:200, 20 min), and streptofluor 594 (1:200, 90 min). Tissue was incubated in a second primary antibody for 48 hr, rinsed in KPBS and exposed to appropriate AlexaFluor secondary antibody for 1 hr. Second primary antibodies included the following: Chemicon, mouse anti-NeuN, 1:50,000; Chemicon, rabbit anti-GAD67/65, 1:30,000; Sigma, rabbit anti-Parvalbumin, 1:30,000; Swant, mouse anti-Calbindin-D28k,1:60,000; Molecular Probes, mouse anti-COX, 1:12,000; rabbit anti-GFAP, Dako 1:25,000; Chemicon, rabbit anti-NG2, 1:1,000; Wako, rabbit anti-Iba-1, 1:9,000; and Abcam, mouse anti-CNPase, 1:20,000. Where two primaries from the same host species were used, tissue was blocked with 0.1 % normal mouse serum and $F(ab)^2$ fragments (1:8,000) prior to incubation in the second primary antibody. Three to five sections were examined for each brain region with positive immunoreactivity. The sections were examined with Nikon Eclipse E800 microscope, using brightfield optics for NiDAB stained sections and with E600W microscope equipped with confocal cell imaging system CARV with appropriate filters for the fluorochrome-treated sections. As a control the staining procedure was repeated with omission of the primary antibody, resulting in the absence of any specific labeling. For double labeling controls we treated tissue with one of the two primaries followed by sequential incubation in each appropriate secondary. This procedure confirmed the specificity of each antibody used in this study.

Western blotting

Immunoblot analysis was performed according to the method described previously (Kristian et al. 2006). Aliquots of isolated non-synaptic and synaptic mitochondria (5 !g protein) were separated by sodium dodecyl sulfate-polyacrylamide gel electrophoresis (SDS-PAGE). To compare the relative levels of cypD between different brain regions, crude mitochondrial samples were purified from homogenates of dissected brain tissues. Non-synaptic, synaptic and crude mitochondrial samples were mixed with lysis buffer (0.5 % NONIDET P-40, 1 % Triton X-100, 150 mM NaCl, 10 mM Tris pH 7.4) and sonicated for 30 sec (Sonicator 3000, Misonix Inc., Farmingdale, NY, USA). Five !g protein was used for loading each lane of the SDS-PAGE gels. After the transfer to polyvinylidene fluoride (PVDF) membranes (Invitrogen), the membranes were washed with phosphate-buffered saline with 0.05 % Tween 20 (PBST) and fixed in a 0.1 % glutaraldehyde in PBST for 10 min. The membranes were washed and incubated in 5 % non-fat milk in PBST for 2 hr, then incubated overnight at 4 °C with monoclonal antibody for cyclophilin D (1:10,000) and for porin (VDAC) (1:10,000) (Mitosciences, LLC). This was followed by washing the membranes in PBST and incubation for 2 hr in HRP-conjugated anti-mouse IgG (1:10,000) (Cell Signaling Technology) antibody. Immunoreactive bands were visualized using the enhanced chemiluminescent detection reagents (Amersham Biosciences). Optical densities of individual bands were quantified after subtraction of background levels of film exposure using the GelExpert software program (Nucleotech, San Carlos, CA, USA).

Isolation of brain mitochondria

Non-synaptic brain mitochondria were isolated according to (Sims 1990) with slight modifications (see (Kristian et al. 2002). Briefly, brains were rapidly removed and

homogenized in ice-cold isolation medium (225 mM mannitol, 75 mM sucrose, 1 mM EGTA, 5 mM Hepes-Tris pH 7.4 at 4 ºC). The brain homogenate was centrifuged at 1,300 g for 3 min. After removing the supernatant, the pellet was resuspended in the isolation medium and centrifuged again at 1,300 g for 3 min. The supernatant was then combined with the supernatant from the previous spin and centrifuged at 17,000 g for 10 min. The resulting pellet was resuspended in 15 % Percoll and layered on top of a discontinuous Percoll gradient (40 %, 24 %). Following centrifugation of the gradient at 32,000 g for 8 min, the mitochondria sedimented at the lower interface between 40 % and 24 % Percoll. The synaptosomes accumulated below the interface of 24 and 15 % Percoll. The nonsynaptic mitochondria were collected and diluted in isolation medium (1:5 vol/vol). After centrifugation at 17,000 g for 10 min, the pellet was resuspended in isolation medium containing 10 mg/ml of defatted bovine serum albumin (BSA) and centrifuged at 7,000 g for 10 min. The synaptosomes were collected and diluted with isolation medium (1:1 vol/vol) and the mitochondria were released from synaptosomes using a nitrogen cavitation technique (Kristian et al. 2006). The suspension was layered on to 24% Percoll and then centrifuged at 32,000 g for 8 min. The synaptic mitochondria that sedimented at the bottom of the tube were collected and diluted in isolation medium (1:5 vol/vol). Following centrifugation, the pellet was resuspended in BSA-containing medium and centrifuged at 7,000 g for 10 min. The final mitochondrial pellet was resuspended in 0.5 ml of lysis buffer.

The crude mitochondrial sample from dissected brain regions of cortex, striatum and substantria nigra were prepared by homogenization of brain tissue that was followed by low speed centrifugation at 1,300 g for 3 min. The supernatant was then centrifuged at 17,000 g for 10 min. The obtained pellet was resuspended in isolation medium and centrifuged again at 7,000 g for 10 min. The final crude mitochondrial pellet was diluted in lysis buffer.

Data Analysis

Statistical differences among different groups were determined using one-way ANOVA followed by Scheffe's F-test. A paired t-test was used to assess the difference in cypD levels between synaptic and non-synaptic mitochondrial samples. Differences with P-values of <0.05 were considered to be statistically significant. All errors are given as standard error of the mean (SEM).

Results

Since the distribution of cypD throughout the brain is unknown, we initially performed an entire rostral to caudal qualitative screen every 12^{th} section for the immunohistochemical detection of cypD positive cells. For the purposes of this study, we focused on only those areas showing the highest number of cells with specific cypD immunoreactivity indicated by a black insoluble deposit at the site of the antigen. The immunoreactivity observed in neuronal cells appeared in two primary patterns. In the first, a zone of punctate staining was observed uniformly around the nucleus (Fig 1 E). In the second, a more intense punctate somatic staining was observed diffusely throughout most of the cytoplasm and extended into one or more dendritic processes (Fig 1 O). Neurons exhibiting both patterns of staining were estimated from each region and included in the relative number of positive cells per $300\mu m^2$ reported in Table 1.

At low magnification, cypD immunostaining was localized predominantly in neurons within the hippocampus, striatum, cortex, septum, substantia nigra (SNr), ventral tegmental area (VTA) and lateral mammillary nucleus (LMN) (see Table 1).

Within the hippocampus, clear immunoreactivity was observed in the pyramidal cell layer with strongly stained neurons scattered throughout both cellular and molecular layers (Fig 1

A–E). Generally, staining in stratum moleculare of all hippocampal subregions was consistently intense (Fig 1 D). The basal dendritic (stratum oriens) layers appeared more immunoreactive than the proximal apical dendritic layer. The immunoreactivity observed within stratum moleculare was moderate, compared to cellular layers. At higher magnification, individual neurons with densely punctate labeling in their cytoplasm, dendrites and glia-like processes (Fig 1 O and P), were interspersed with the neurons exhibiting a granular staining pattern only in the neuropil and somata. Staining was also evident within non-neuronal cell types within these regions.

Other brain regions displaying neurons with strong cypD immunoreactivity were cortex, striatum, septum, SNr, VTA and the LMN (Fig 1 F–N). Cortical neuron staining was heterogeneous, localized primarily in perinuclear regions and in the proximal segment of axons. Neurons with stronger staining were scattered within the laminae II, III, IV and VI (Fig 1 G) mainly in the frontal cortex. Moderately stained neurons were also observed in the parietal cortex. Strongly labeled neurons were localized in the posterior piriform cortex (Fig 1 I). These neurons show intense punctated staining in perinuclear regions. In this area of the cortex there is also a spotted immunostaining of small cells with a non-neuronal morphology (Fig 1 I). Caudate putamen displayed a scattered immunoreactivity with strongly stained medium sized spiny cells (Fig 1 H). Similarly, VTA, SNr and LMN neurons with spiny somas and dendrites were clearly cypD immunoreactive (Fig 1 K–M). Strong reactive neurons were localized in septal regions with mostly perinuclear staining (Fig 1 N). Little to no staining was observed in several brain regions including the cerebellum, nucleus accumbens, corpus callosum, cortical layer I and geniculate nucleus.

Since cypD is a mitochondrial protein we used cytochrome oxidase (COX) subunit I antibody to confirm mitochondrial localization of the cypD staining. Fig 2 (A–C) demonstrates co-localization of COX and cypD immunoreactivity. To determine which non-neuronal cell types expressed cypD immunoreactivity, tissue was co-labeled with antibodies against glial markers for astrocytes (GFAP and S100β), microglia (Iba1), oligodendrocytes (CNPase) and synantocytes (cells expressing NG2 chondroitin sulphate proteoglycan) (for review see (Butt et al. 2005). There was no clear overlap between cypD immunoreactivity and microglial or oligodendrocyte markers. However, double labeling with GFAP and S100β staining revealed a subset of mitochondria in astrocytes expressing high levels of cypD. A clear cypD signal was present in the thick proximal processes of the GFAP or S100β–labeled astrocytes (Fig 2 D–I). Similarly, mitochondria in a sub-population of NG2 cells within piriform cortex and hippocampal regions showed strong immunoreactivity to cypD, particularly in perinuclear regions (Fig 2 J–L).

To confirm quantitative differences in cypD levels between various brain regions and cell types, we isolated mitochondria from regions showing strong immunoreactivity, analyzed cypD levels by western immunoblots, and quantified the individual cypD band intensities. Typical examples of immunoreactivity to cypD of mitochondrial samples obtained from cortex, striatum and substantia nigra are shown in Fig 3A. The immunoreactivity to VDAC (a mitochondrial outer membrane protein) was used as a loading control. The content of cypD was 40–50 % higher in the SNr mitochondrial fraction when compared to the cortical sample and 33% higher when compared to mitochondria from the striatum (Fig 3B). In non-synaptic mitochondria (representing mitochondria from glia and neuronal cell bodies) the cypD level was 16 % higher than in the synaptic fraction (representing mitochondria from neuron terminals).

The morphology and distribution of neurons with high cypD immunoreactivity in most brain regions resembles GABAergic interneurons. These GABAergic interneurons are characterized by knotted dendrites and the expression of glutamic acid decarboxylase

(GAD) and high levels of the calcium binding proteins parvalbumin or calbindin. We therefore examined whether neurons with strong cypD immunoreactivity also showed positive staining with markers of GABAergic cells. As fig 4 shows, there is a clear overlap of GAD and cypD immunostaining in the septal area (Fig 3A–C), in caudate putamen (Fig 4D–F), in cells of hippocampal regions (Fig 4G–I), and throughout the substantia nigra (Fig 4J–L). Similarly, immunoreactivity to parvalbumin was co-localized with cypD positive staining in a subset of hippocampal neurons (Fig 5A–C), in neurons of the mammillary nucleus (Fig 5D–F), and piriform cortex (Fig 5G–I). CypD positive neurons in cortex also expressed high levels of calbindin-D28k (Fig 5K–M). Taken together these data suggest GABAergic interneurons are in fact one of the richest sources of mitochondrial cypD in the adult rodent brain.

Discussion

The results from this study demonstrate that different levels of the mitochondrial matrix protein cyclophilin D (cypD) exist within various brain regions as well as between different cell-types. CypD immunostaining in individual cells was punctate and localized generally in perinuclear regions and in proximal dendrites. Interestingly, the cypD distribution within the hippocampus was similar to the distribution of cytochrome oxidase (COX) and cytochrome c (cyt c) (Kageyama 1982; Chandrasekaran et al. 2006, see also Naga 2007). However, although the cypD immunoreactivity within the pyramidal cell layer was homogenous, cells with particularly strong positive staining where scattered throughout the hippocampus. The distribution pattern of strongly labeled neurons suggested that high levels of cypD were expressed in a subpopulation of GABAergic interneurons. Double staining with cypD and markers of interneurons (GAD, PV, or calbindin-D28k) revealed that the neurons with high cypD immunoreactivity express GAD and mostly PV. In addition to neurons, non-neuronal cells demonstrated positive immunoreactivity to cypD (see also Naga 2007). These cells represent a subset of astrocytes and NG2 cells. The presence of the cypD signal in the thick proximal processes of astrocytes was similar to distribution of cyt c in astrocytes (Gulyas et al. 2006).

High immunoreactivity within individual cells can be a result of either selectively higher expression of cypD or simply due to a greater number of mitochondria in these cells. Fluorescence staining revealed that the stained organelles were brighter in positive cells rather than occurring in greater numbers when compared to cells with low immunoreactivity, suggesting higher levels of the cypD in individual mitochondria.

Cells with intense cypD staining in Str, Sep, SNr, VTA and cortex also co-expressed GAD and calcium binding proteins, characteristic of interneurons (for review see Celio 1990). Unlike in the hippocampus, most of the cypD positively stained cortical neurons expressed high levels of calbindin-D28k. In the substantia nigra positive cypD immunoreactivity was present in interneurons and also enriched in cells within the pars reticulara suggesting increased cypD levels in dopaminergic neurons.

These data suggest that in all brain regions with strong cypD immunostaining, high levels of cypD are expressed in GABAergic interneurons. In general, interneurons, particularly the one expressing PV, are the most active cells showing high discharge rates (Csicsvari et al. 1999, Pawelzik et al. 2002, Klausberger et al. 2005). The high energy demand of these cells is reflected in higher levels of mitochondrial respiratory enzymes (McCasland and Hibbard 1997, Attwell and Laughlin 2001) requiring faster turnover of mitochondrial proteins. Therefore the higher levels of cypD could be the results of a need for faster refolding of newly imported proteins (Schatz 1996).

The quantitative comparison of the cypD levels between non-synaptic mitochondria, enriched with those from glia and neuronal cell bodies, and synaptic mitochondria, enriched with those from nerve terminals, indicates that the non-synaptic fraction possess higher levels of cypD. This finding is not in agreement with the conclusion of Naga and colleagues (Naga 2007), who reported higher levels of cypD in synaptic mitochondria when compared to a non-synaptic subpopulation. A possible explanation for this discrepancy could be that our western blot protocol includes fixing of the PVDF membrane with glutaraldehyde after transfer of proteins from the SDS gel. This procedure greatly enhances detection of cypD by preventing the loss of the proteins from the membrane during blotting with antibodies and washing procedures (Connern and Halestrap 1992). The non-synaptic fractions used in our immunoblots contain mitochondria primarily from perinuclear regions of neurons and glia that also demonstrate strong immunoreactivity to cypD. The immunoreactivity to cypD of mitochondria located in distal processes and synaptic endings was very weak. Thus, our western blot results are in agreement with our immunohistochemistry findings. Similarly, the immunoblots confirmed higher levels of cypD in SNr when compared to cortex. Striatum showed a tendency toward increased levels of cypD compared to cortex but the difference was not significant (however, see Brustovetsky et al. 2003). Relative low levels of cypD immunoreactivity in cerebellum, nucleus accumbebs or corpus callosum can be a consequence of lower cyclophilins mRNA levels in these brain regions (see Lad et al. 1991).

Our finding that mitochondria preferentially in interneurons contain high levels of cypD has important implications for in vitro studies with isolated brain mitochondria, particularly when the MPT is examined. Brain mitochondria show a very heterogeneous response to MPT-inducing agents. Our data suggest that this heterogeneous response of isolated brain mitochondria to the insult can be due to the different cypD levels in various sub-populations of brain mitochondria. Thus, a sub-population of isolated mitochondria originating particularly from interneurons will be most sensitive while the rest of the mitochondrial population will be more resistant to calcium – induced MPT. Interneurons represent about 15–30% of all cortical neurons (Parnavelas et al. 1977; Hendry et al. 1987); Meinecke and Peters 1987). Since non-synaptic mitochondria include both mitochondria originated from neurons and glia the fraction of interneuronal mitochondria is probably less than 15%. Interestingly, this conclusion is in agreement with the finding that only about 10 % of isolated non-synaptic mitochondria display typical signs of swelling (damaged cristae with low electron density and disrupted membranes) when exposed to high levels of calcium (Kristian et al. 2002). However, other factors can also affect mitochondrial sensitivity to calcium. For example the endogenous levels of adenine nucleotides modulate the calcium-induced swelling of brain mitochondria (Friberg et al. 1999). Although our findings show relatively low immunoreactivity of cypD in cerebellum when compared to cortex the higher resistance of cerebellar mitochondria to calcium-induced damage seems to be more a result of higher endogenous adenine nucleotides levels in these mitochondria when compared to cortical one (Friberg et al. 1999).

The effect of cypD levels on sensitivity to MPT pore opening were also shown during development (Eliseev et al. 2006). In newborn rats, sensitivity of brain mitochondria to the MPT and cypD expression is significantly higher then in mature animals. Thus, the lower expression of cypD in adult animals increased the calcium threshold of brain mitochondria to the MPT (Eliseev et al. 2006). Taken together, one needs to exercise caution when studying MPT in isolated brain mitochondria since only a small population of mitochondria from interneurons will show high sensitivity to calcium-induced damage while the rest of the mitochondrial population does not show typical signs of MPT.

Acknowledgments

This work was supported by National Institute of Health Grants R21NS050653 (T.K.), R21NS058556 (T.K.), and NS34152 (G.F.).

References

Andreyev A, Fiskum G. Calcium induced release of mitochondrial cytochrome c by different mechanisms selective for brain versus liver. Cell Death Differ. 1999; 6(9):825–832. [PubMed: 10510464]

Attwell D, Laughlin SB. An energy budget for signaling in the grey matter of the brain. J Cereb Blood Flow Metab. 2001; 21(10):1133–1145. [PubMed: 11598490]

Basso E, Fante L, Fowlkes J, Petronilli V, Forte MA, Bernardi P. Properties of the permeability transition pore in mitochondria devoid of Cyclophilin D. J Biol Chem. 2005; 280(19):18558–18561. [PubMed: 15792954]

Bernardi P, Vassanelli S, Veronese P, Colonna R, Szabo I, Zoratti M. Modulation of the mitochondrial permeability transition pore. Effect of protons and divalent cations. J Biol Chem. 1992; 267(5): 2934–2939. [PubMed: 1737749]

Brown MR, Sullivan PG, Geddes JW. Synaptic mitochondria are more susceptible to Ca2+overload than nonsynaptic mitochondria. J Biol Chem. 2006; 281(17):11658–11668. [PubMed: 16517608]

Brustovetsky N, Brustovetsky T, Purl KJ, Capano M, Crompton M, Dubinsky JM. Increased susceptibility of striatal mitochondria to calcium-induced permeability transition. J Neurosci. 2003; 23(12):4858–4867. [PubMed: 12832508]

Brustovetsky N, Dubinsky JM. Limitations of cyclosporin A inhibition of the permeability transition in CNS mitochondria. J Neurosci. 2000; 20(22):8229–8237. [PubMed: 11069928]

Butt AM, Hamilton N, Hubbard P, Pugh M, Ibrahim M. Synantocytes: the fifth element. J Anat. 2005; 207(6):695–706. [PubMed: 16367797]

Celio MR. Calbindin D-28k and parvalbumin in the rat nervous system. Neuroscience. 1990; 35(2): 375–475. [PubMed: 2199841]

Chandrasekaran K, Hazelton JL, Wang Y, Fiskum G, Kristian T. Neuron-specific conditional expression of a mitochondrially targeted fluorescent protein in mice. J Neurosci. 2006; 26(51): 13123–13127. [PubMed: 17182763]

Connern CP, Halestrap AP. Purification and N-terminal sequencing of peptidyl-prolyl cis-trans-isomerase from rat liver mitochondrial matrix reveals the existence of a distinct mitochondrial cyclophilin. Biochem J. 1992; 284(Pt 2):381–385. [PubMed: 1599421]

Crompton M. On the involvement of mitochondrial intermembrane junctional complexes in apoptosis. Curr Med Chem. 2003; 10(16):1473–1484. [PubMed: 12871121]

Crompton M, Barksby E, Johnson N, Capano M. Mitochondrial intermembrane junctional complexes and their involvement in cell death. Biochimie. 2002; 84(2–3):143–152. [PubMed: 12022945]

Csicsvari J, Hirase H, Czurko A, Mamiya A, Buzsaki G. Oscillatory coupling of hippocampal pyramidal cells and interneurons in the behaving Rat. J Neurosci. 1999; 19(1):274–287. [PubMed: 9870957]

Dubinsky JM, Brustovetsky N, Pinelis V, Kristal BS, Herman C, Li X. The mitochondrial permeability transition: the brain's point of view. Biochem Soc Symp. 1999; 66:75–84. [PubMed: 10989659]

Eliseev RA, Filippov G, Velos J, Vanwinkle B, Goldman A, Rosier RN, Gunter TE. Role of cyclophilin D in the resistance of brain mitochondria to the permeability transition. Neurobiol Aging. 2006

Friberg H, Connern C, Halestrap AP, Wieloch T. Differences in the activation of the mitochondrial permeability transition among brain regions in the rat correlate with selective vulnerability. J Neurochem. 1999; 72(6):2488–2497. [PubMed: 10349859]

Gothel SF, Marahiel MA. Peptidyl-prolyl cis-trans isomerases, a superfamily of ubiquitous folding catalysts. Cell Mol Life Sci. 1999; 55(3):423–436. [PubMed: 10228556]

Griffiths EJ, Halestrap AP. Further evidence that cyclosporin A protects mitochondria from calcium overload by inhibiting a matrix peptidyl-prolyl cis-trans isomerase. Implications for the

immunosuppressive and toxic effects of cyclosporin. Biochem J. 1991; 274(Pt 2):611–614. [PubMed: 1706598]

Gulyas AI, Buzsaki G, Freund TF, Hirase H. Populations of hippocampal inhibitory neurons express different levels of cytochrome c. Eur J Neurosci. 2006; 23(10):2581–2594. [PubMed: 16817861]

Gunter TE, Pfeiffer DR. Mechanisms by which mitochondria transport calcium. Am J Physiol. 1990; 258(5 Pt 1):C755–786. [PubMed: 2185657]

Halestrap AP, Davidson AM. Inhibition of Ca2(+)-induced large-amplitude swelling of liver and heart mitochondria by cyclosporin is probably caused by the inhibitor binding to mitochondrial-matrix peptidyl-prolyl cis-trans isomerase and preventing it interacting with the adenine nucleotide translocase. Biochem J. 1990; 268(1):153–160. [PubMed: 2160810]

Halestrap AP, McStay GP, Clarke SJ. The permeability transition pore complex: another view. Biochimie. 2002; 84(2–3):153–166. [PubMed: 12022946]

Hendry SH, Schwark HD, Jones EG, Yan J. Numbers and proportions of GABA-immunoreactive neurons in different areas of monkey cerebral cortex. J Neurosci. 1987; 7(5):1503–1519. [PubMed: 3033170]

Kageyama GW-RMT. Histochemical localization of cytochrome oxidase in the hippocampus: correlation with specific neuronal types and afferent pathways. Neuroscience. 1982; 7(10):2337–2361. [PubMed: 6294558]

Klausberger T, Marton LF, O'Neill J, Huck JH, Dalezios Y, Fuentealba P, Suen WY, Papp E, Kaneko T, Watanabe M, Csicsvari J, Somogyi P. Complementary roles of cholecystokinin- and parvalbumin-expressing GABAergic neurons in hippocampal network oscillations. J Neurosci. 2005; 25(42):9782–9793. [PubMed: 16237182]

Kristal BS, Dubinsky JM. Mitochondrial permeability transition in the central nervous system: induction by calcium cycling-dependent and -independent pathways. J Neurochem. 1997; 69(2): 524–538. [PubMed: 9231710]

Kristal BS, Staats PN, Shestopalov AI. Biochemical characterization of the mitochondrial permeability transition in isolated forebrain mitochondria. Dev Neurosci. 2000; 22(5–6):376–383. [PubMed: 11111153]

Kristian T, Bernardi P, Siesjo BK. Acidosis promotes the permeability transition in energized mitochondria: implications for reperfusion injury. J Neurotrauma. 2001; 18(10):1059–1074. [PubMed: 11686493]

Kristian T, Gertsch J, Bates TE, Siesjo BK. Characteristics of the calcium-triggered mitochondrial permeability transition in nonsynaptic brain mitochondria: effect of cyclosporin A and ubiquinone O. J Neurochem. 2000; 74(5):1999–2009. [PubMed: 10800943]

Kristian T, Hopkins IB, McKenna MC, Fiskum G. Isolation of mitochondria with high respiratory control from primary cultures of neurons and astrocytes using nitrogen cavitation. J Neurosci Methods. 2006; 152(1–2):136–143. [PubMed: 16253339]

Kristian T, Pivovarova NB, Fiskum G, Andrews SB. Calcium-induced precipitate formation in brain mitochondria: composition, calcium capacity, and retention. J Neurochem. 2007; 102(4):1346–1356. [PubMed: 17663756]

Kristian T, Weatherby TM, Bates TE, Fiskum G. Heterogeneity of the calcium-induced permeability transition in isolated non-synaptic brain mitochondria. J Neurochem. 2002; 83(6):1297–1308. [PubMed: 12472884]

Lad RP, Smith MA, Hilt DC. Molecular cloning and regional distribution of rat brain cyclophilin. Brain Res Mol Brain Res. 1991; 9(3):239–244. [PubMed: 1851525]

Larsson E, Lindvall O, Kokaia Z. Stereological assessment of vulnerability of immunocytochemically identified striatal and hippocampal neurons after global cerebral ischemia in rats. Brain Res. 2001; 913(2):117–132. [PubMed: 11549375]

Li Y, Johnson N, Capano M, Edwards M, Crompton M. Cyclophilin-D promotes the mitochondrial permeability transition but has opposite effects on apoptosis and necrosis. Biochem J. 2004; 383(Pt 1):101–109. [PubMed: 15233627]

Matouschek A, Rospert S, Schmid K, Glick BS, Schatz G. Cyclophilin catalyzes protein folding in yeast mitochondria. Proc Natl Acad Sci U S A. 1995; 92(14):6319–6323. [PubMed: 7603990]

McCasland JS, Hibbard LS. GABAergic neurons in barrel cortex show strong, whisker-dependent metabolic activation during normal behavior. J Neurosci. 1997; 17(14):5509–5527. [PubMed: 9204933]

Meinecke DL, Peters A. GABA immunoreactive neurons in rat visual cortex. J Comp Neurol. 1987; 261(3):388–404. [PubMed: 3301920]

Naga KSPG, Geddes JW. High cyclophilin D content of synaptic mitochondria results in increased vulnerability to permeability transition. Journal of Neuroscience. 2007; 27(28):7469–7475. [PubMed: 17626207]

Nicolli A, Basso E, Petronilli V, Wenger RM, Bernardi P. Interactions of cyclophilin with the mitochondrial inner membrane and regulation of the permeability transition pore, and cyclosporin A-sensitive channel. J Biol Chem. 1996; 271(4):2185–2192. [PubMed: 8567677]

Parnavelas JG, Lieberman AR, Webster KE. Organization of neurons in the visual cortex, area 17, of the rat. J Anat. 1977; 124(Pt 2):305–322. [PubMed: 591429]

Pawelzik H, Hughes DI, Thomson AM. Physiological and morphological diversity of immunocytochemically defined parvalbumin- and cholecystokinin-positive interneurones in CA1 of the adult rat hippocampus. J Comp Neurol. 2002; 443(4):346–367. [PubMed: 11807843]

Rospert S, Looser R, Dubaquie Y, Matouschek A, Glick BS, Schatz G. Hsp60-independent protein folding in the matrix of yeast mitochondria. EMBO J. 1996; 15(4):764–774. [PubMed: 8631298]

Schatz G. The protein import system of mitochondria. J Biol Chem. 1996; 271(50):31763–31766. [PubMed: 8943210]

Schmid FX. Prolyl isomerase: enzymatic catalysis of slow protein-folding reactions. Annu Rev Biophys Biomol Struct. 1993; 22:123–142. [PubMed: 7688608]

Schmid FX. Protein folding. Prolyl isomerases join the fold. Curr Biol. 1995; 5(9):993–994. [PubMed: 8542292]

Sims NR. Rapid isolation of metabolically active mitochondria from rat brain and subregions using Percoll density gradient centrifugation. J Neurochem. 1990; 55(2):698–707. [PubMed: 2164576]

Watson RE Jr, Wiegand SJ, Clough RW, Hoffman GE. Use of cryoprotectant to maintain long-term peptide immunoreactivity and tissue morphology. Peptides. 1986; 7(1):155–159. [PubMed: 3520509]

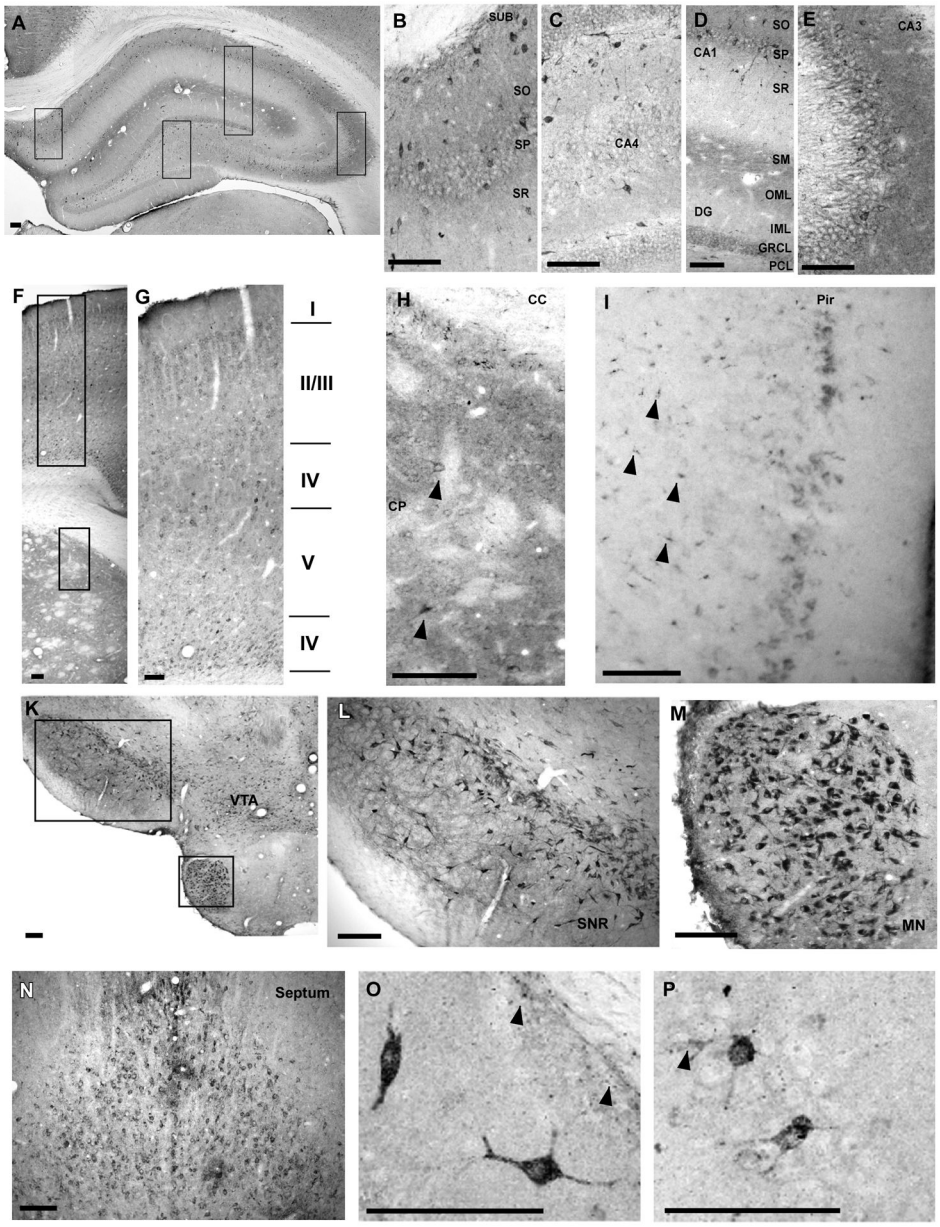

Fig. 1.

Regional distribution of cypD within different brain regions. Hippocampus (A–E). The intensity of staining within the cellular layers is highest in CA3 (E) followed by subicculum (B), CA1 and dentate gyrus (D). Furthermore, the immunoreactivity is particularly high above and below the hippocampal fissure and within the cellular and basal dendritic layers of CA3. There are scattered cells with intense staining throughout all hippocampal regions. Panels B–E are enlarged images taken from panel as shown by black boxes. Caudate putamen and overlaying cortex (F–H). Intense immunoreactivity within caudate putamen with scattered strongly stained neurons (arrowheads) (H). Strongly stained neurons are localized particularly in cortical layers II/IV and VI (G). Neurons with high cypD immunoreactivity were also localized in layer I of Piriform cortex. Furthermore, non-neuronal cells in deeper layers within this region were also strongly stained (arrowheads). Substantia nigra (SNr), ventral tagmental area (VTA), mammilary nucleus (MN) (K, L, M)

and septum (N) contained neurons with intense staining. Panel O and P demonstrate individual neurons within the CA1 (O) and the CA3 (P) sector of the hippocampus with high immunoreactivity. Arrowheads indicate non-neuronal cells with high cypD staining. Scale bar = 100 μm.

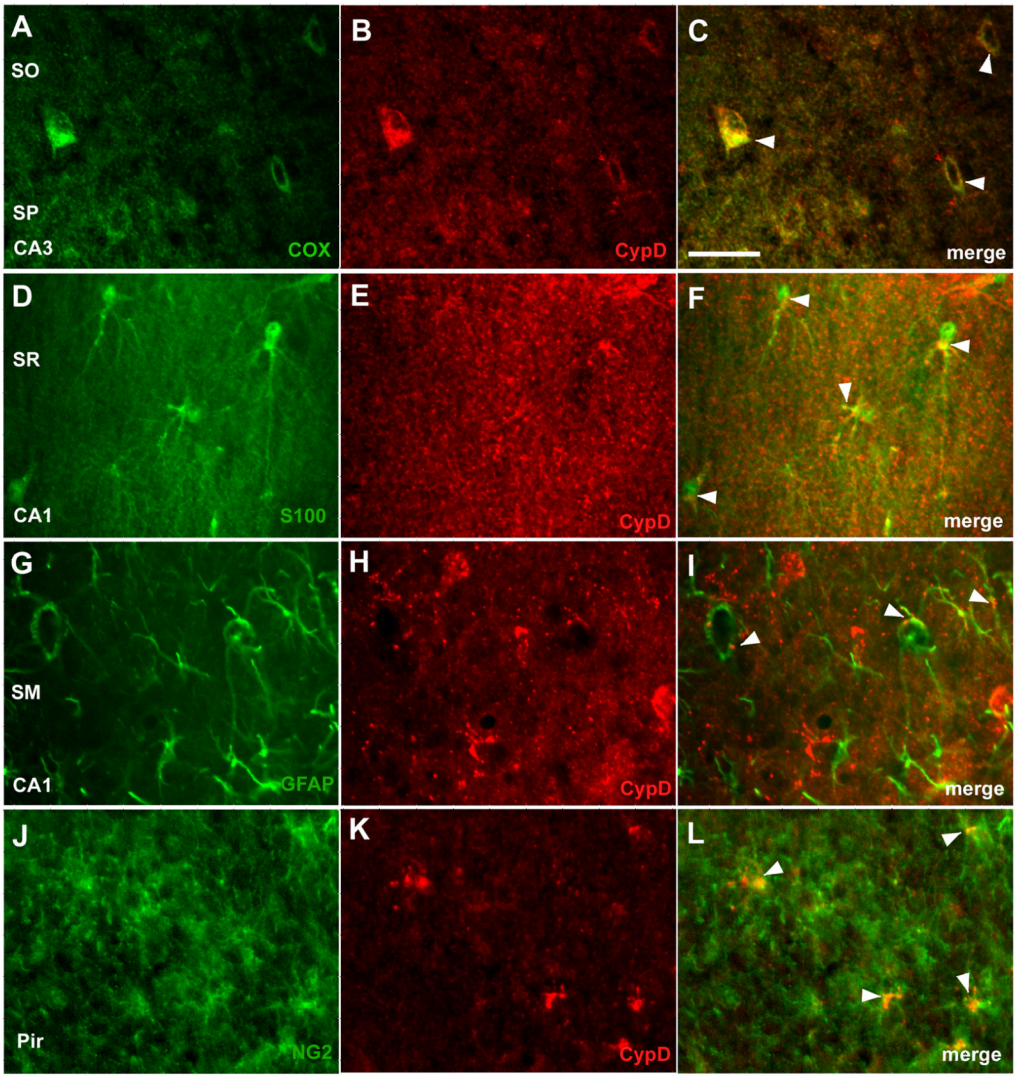

Fig. 2.

Localization of cypD immunoreactivity in mitochondria and cell-type specific expression. A–C double immunolabeling with anti-cypD (red) and anti-COX (green). Co-expression of cypD and COX (C) (arrowhead) confirmed cypD localization in mitochondria. Double staining of hippocampal area with anti-cypD and astrocyte markers; anti-S100β(D–F) and anti-GFAP (G–I). Most of the astrocytes show intense punctate staining. Anti-NG2 and anti-cypD immunolabeling of piryform cortex (J–L). Scale bar = 50 μm.

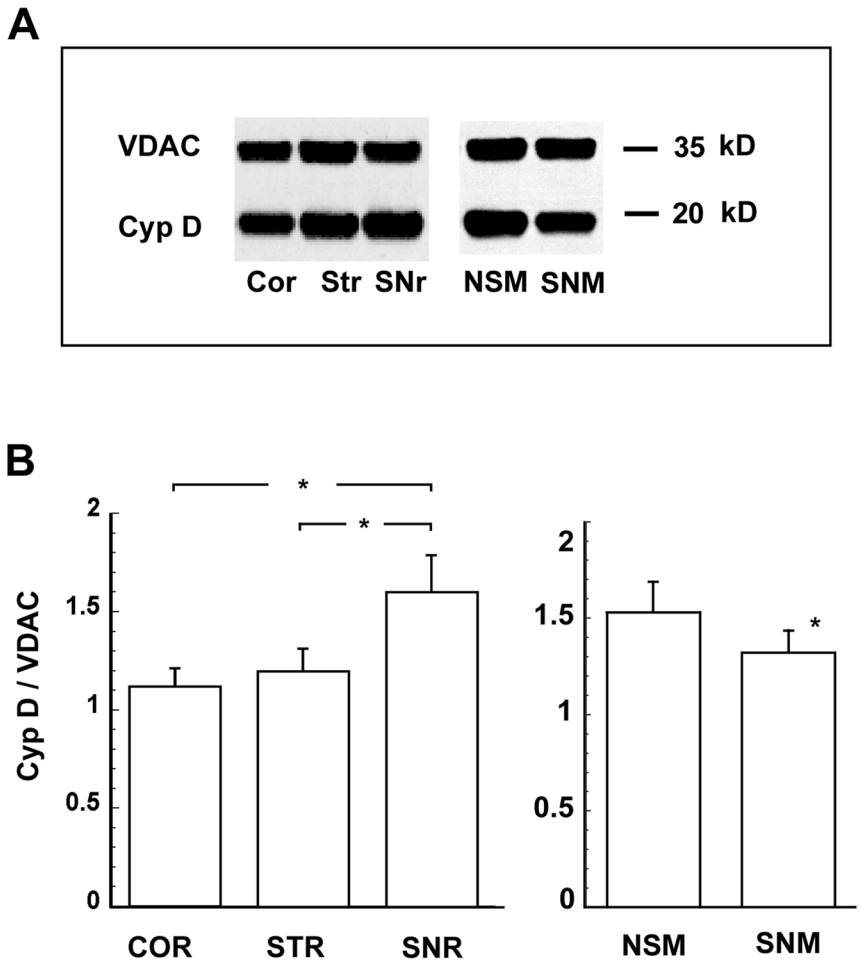

Fig. 3.

Relative distribution of cypD in crude mitochondrial samples from different brain regions and in non-synaptic and synaptic mitochondria. Cyclophilin D immunoreactivity was normalized to the VDAC signal. The normalized immunoreactivity is significantly higher in substantia nigra (SNr) when compared to cortex (Cor) and striatum (Str) ($p < 0.05$, $n = 4$)(A). Non-synaptic mitochondria (NSM) demonstrated significantly higher levels of cypD when compared to synaptic mitochondria (SNM) ($p < 0.05$, $n = 6$) (B).

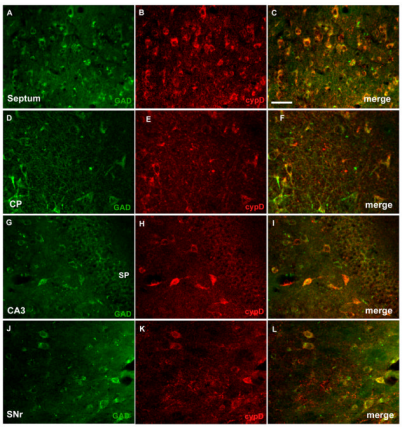

Fig. 4.

CypD is highly expressed in GABA-ergic interneurons. Double staining with anti-cypD (red) and anti-GAD (green) of septum (A–C), caudate putamen (CP)(D–F), CA3 region of the hippocampus (G–I), and substantia nigra (SNr)(J–L). The merged images demonstrate that neurons with high cypD immunoreactivity express glutamate decarboxylase (GAD). Scale bar = 50 μm.

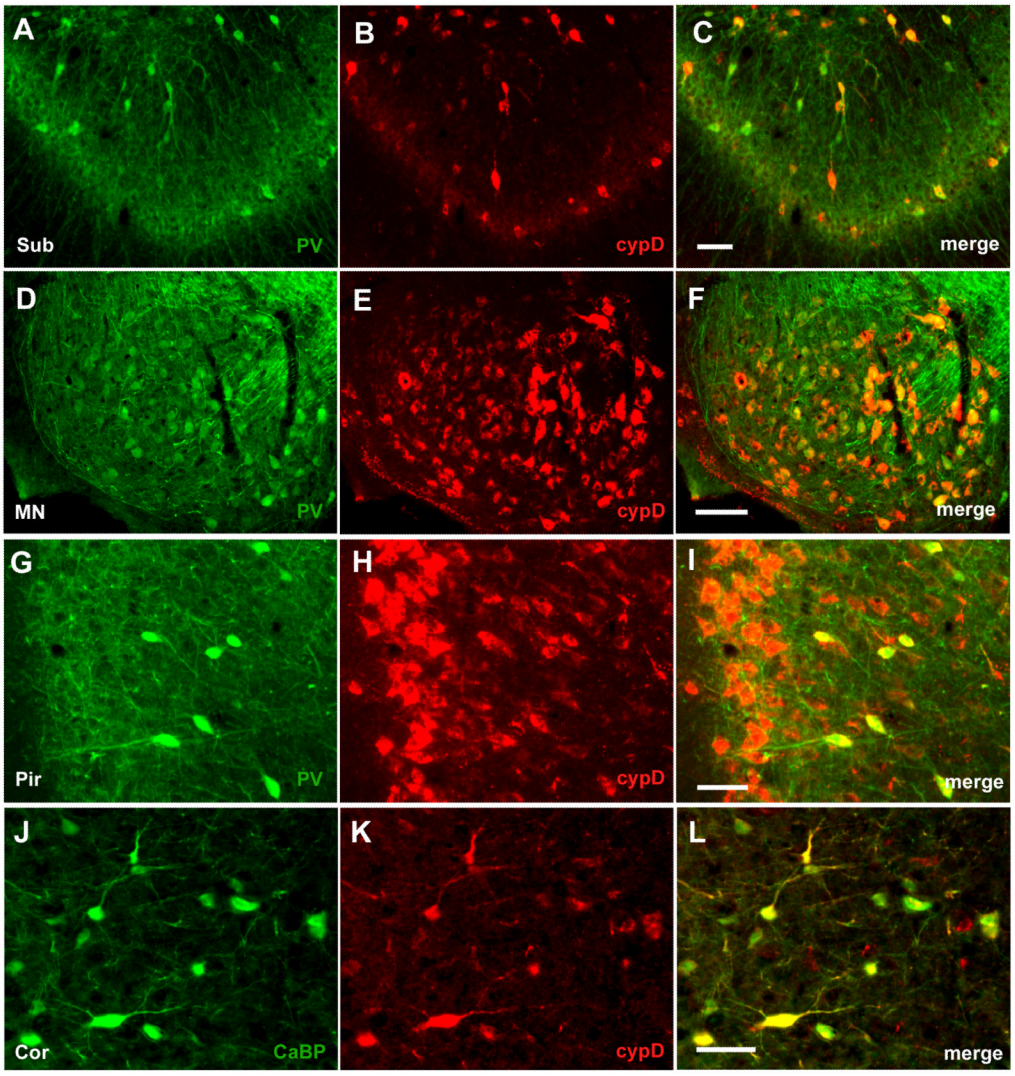

Fig. 5.

Co-expression of calcium binding proteins parvalbumin (PV) and calbindin-28kD (CaBP) with cypD. Most of the hippocampal neurons with high immunoreactivity to cypD (red) expressed parvalbumin (green) (A–C). Similarly positively stained neurons in mammilary nucleus (MN) (D–F), and sub-population of neurons in deeper layers of pyriform cortex (Pyr)(G–I) also contained parvalbumin. Cortical neurons with strong immunoreactivity to cypD expressed calbindin 28kD (J–L). Scale bar = 50 μm.

Table 1

Relative number of neurons with positive cypD immunoreactivit y within different brain regions.

Brain region	Immunoreactive neurons per 300 μm^2 (P + PD)	Strongly stained neurons % (PD)
Hippocampus CA1	+	0–25
Hippocampus CA3	+ +	0–25
Dentate gyrus	+ +	0–25
Subiculum	+	0–25
Caudate putamen	+ +	0–25
Septum	+ + + +	50–75
Nucleus accumbens	+	0
Cortex - frontal	+ + +	0–25
Cortex - Piriform	+ +	25–50
Substantia Nigra	+ +	75–100
Ventral tegmental area	+ + +	75–100
Mamillary nucleus	+ + + +	75–100
Corpus callosum	−	0

P - neurons showing cypD immunorectivity only in perikaryal region

PD - neurons with positive staining in both perikaryal region and proximal dendrites

The data are estimated from bilateral cell counts in a randomly selected 300 × 300 μm counting frame within a given region.

− = no cells present, + = 1–15 cells,

++ = 15–50 cells,

+++ = 50 – 100 cells,

++++ < 100 cells/300 μm^2.

Percentages represent the percent of the PD type neurons of all positively stained cells.